J. Fluid Mech. (2002), *vol.* 459, *pp.* 289–306.
DOI: 10.1017/S0022112002008224 Printed in the United Kingdom

The effect of surfactant on the stability of a liquid thread

By MARY-LOUISE E. TIMMERMANS† AND JOHN R. LISTER

Institute of Theoretical Geophysics, Department of Applied Mathematics and Theoretical Physics, University of Cambridge, Silver Street, Cambridge CB3 9EW, UK

(Received 18 April 2001 and in revised form 22 August 2001)

The surface-tension-driven motion of a surfactant-coated liquid thread in inviscid surroundings is investigated using linear stability theory as well as one-dimensional nonlinear approximations to the governing Navier–Stokes equations. Examination of analytic limits of the linear dispersion relationship demonstrates that surfactant acts as a distinct mechanism for long-wavelength cut-off, instead of inertia, if the surfactant effects exceed a critical value, $\beta = \frac{1}{2}$, where β is a dimensionless surface-tension gradient. Two different long-wavelength regimes can be identified, depending on the degree of tangential stress, with $\beta = 1$ characterizing a transition from extensionally dominated inertial flow to shear-dominated viscous flow. One-dimensional nonlinear models are formulated which capture the changes in behaviour with variation of β by inclusion of the necessary high-order terms. Scaling close to breakup shows that surfactant is swept away from the pinching region and then has little effect.

1. Introduction

The surface-tension-driven instability of a liquid thread is a well-known problem with applications to many industrial processes, such as ink-jet printing and the manufacture of optical fibres. Theoretical work on the subject stems from Lord Rayleigh's (1879, 1892) classic papers. Rayleigh performed linear stability analyses for both inviscid and viscous threads (in inviscid surroundings) to show that infinitesimal perturbations to a thread will grow if the wavelength of the perturbation is greater than the circumference of the thread. The instability leads to the breakup of the thread into droplets. In a subsequent study, Tomotika (1935) incorporated a viscous surrounding liquid into the analysis to show that very long wavelengths have slower growth rates than for threads in inviscid surroundings because of the greater shear stresses involved in transporting liquid along the thread.

Nonlinear growth of the surface-tension instability leads to the formation of smaller drops (satellite drops) from the thin thread left between main drops. The nonlinear dynamics of thread breakup have been described analytically by the development of one-dimensional approximations to the governing Navier–Stokes equations (Eggers & Dupont 1994; Garcia & Castellanos 1994). The one-dimensional models are based on the assumption that the thread is long and thin, so that flow is mainly in the axial direction and uniform across the thread. Eggers (1997) presents a comprehensive review of nonlinear theories and experimental work on the details of the nonlinear behaviour of the surface-tension instability.

† Present address: Institute of Ocean Sciences, PO Box 6000, Sidney, BC V8L 4B2, Canada.

The surface-tension-driven flow of a surfactant-coated thread, while often of importance to thread breakup problems in industry, is less well-studied than the surfactant-free case. The surface tension of a surfactant-coated thread depends on the concentration of surfactant adsorbed on its surface. If motion of the surface causes variations in the surface concentration then the consequent gradient of surface tension gives rise to a tangential stress on the surface, which itself produces motion. Stone & Leal (1990) and Milliken, Stone & Leal (1993) investigated the deformation and breakup of surfactant-coated drops in an extensional flow in order to develop an understanding of the relationship between flow, surfactant concentration and surface stresses. These studies showed that surfactant retards the growth rate of disturbances to the drop, mainly owing to the effect of surface-tension gradients at the surface, but also to a reduction in the average surface-tension due to the presence of surfactant. Milliken *et al.* (1993) also show that surfactants can have a significant effect on the pattern of breakup of filamental structures such as those produced by mixing flows (Tjahjadi & Ottino 1991).

Whitaker (1976) considered the effects of surfactant on the stability of a liquid thread in inviscid surroundings and showed, for example, that surfactant has no effect upon the minimum wavelength for instability. Palierne & Lequeux (1991) studied the effects of 'surface elasticity' resulting from surface-tension gradients due to the presence of surfactant for general viscoelastic fluids (both the thread and the surrounding fluid) in the Stokes regime. They did not incorporate a surfactant transport equation, nor an equation relating surface tension to surfactant concentration, and hence had to introduce a 'dilatational modulus' to relate surface stresses to surface strains. This assumption is not equivalent to the results of modelling surfactant transport below. In a recent thorough analysis, Hansen, Peters & Meijer (1999) used linear stability theory to investigate the influence of a soluble surfactant on thread breakup when the thread is surrounded by another viscous fluid. They explicitly coupled local fluctuations of surface tension due to the transport of soluble surfactant with the governing Navier–Stokes equations to determine a characteristic equation relating growth rate to wavenumber for a periodically perturbed thread. Kwak & Pozrikidis (2001) extended the analysis of Hansen *et al.* (1999) of the case of insoluble surfactant to include coaxial internal and external rigid boundaries as might occur in coating problems. They also studied the nonlinear evolution towards drop formation in the absence of inertia using the boundary-integral representation of Stokes flow. Ambravaneswaran & Basaran (1999) used a one-dimensional approximation of the full Navier–Stokes equations to examine the nonlinear effects of insoluble surfactant on the breakup of an extending liquid bridge.

In this paper, we investigate in some detail the motion and breakup of a thread of viscous liquid that is coated with insoluble surfactant and is in inviscid surroundings. Our aim is to increase understanding of the role of surfactant by investigation of the limiting forms of the characteristic equation and, thereby, to bring the dominant physical balances into clear focus. We also formulate one-dimensional models to describe the nonlinear flow regimes in more detail, and show that it is necessary to include high-order terms to capture even the linear behaviour.

The paper is organized as follows. In § 2 we summarize the governing axisymmetric Navier–Stokes equations and interfacial boundary conditions, including an evolution equation for the surface surfactant concentration. In § 3 we apply linear stability theory to examine the effects of insoluble surfactant on the dynamics of a long viscous thread. In particular, we investigate long-wavelength limits of the characteristic equation as well as the limiting cases of inviscid and viscous threads and of large

surface-tension-gradient stresses. In § 4 we derive one-dimensional models to describe the nonlinear dynamics that lead to surface-tension-driven breakup of a surfactant-coated thread.

2. Governing equations

We consider perturbations to an axisymmetric cylinder of incompressible liquid of viscosity μ and density ρ. We assume that the effects of gravity and any surrounding fluid are negligible. Insoluble surfactant resides on the surface of the liquid thread. The equation of the surface is given by $r = a(z,t)$ in cylindrical coordinates (r,z) aligned with the thread, where t is time. The radial and axial components of the Navier–Stokes equations are

$$\rho\left(\frac{\partial u}{\partial t}+u\frac{\partial u}{\partial r}+w\frac{\partial u}{\partial z}\right)=-\frac{\partial p}{\partial r}+\mu\left(\frac{\partial^2 u}{\partial r^2}+\frac{\partial^2 u}{\partial z^2}+\frac{1}{r}\frac{\partial u}{\partial r}-\frac{u}{r^2}\right), \tag{2.1}$$

$$\rho\left(\frac{\partial w}{\partial t}+u\frac{\partial w}{\partial r}+w\frac{\partial w}{\partial z}\right)=-\frac{\partial p}{\partial z}+\mu\left(\frac{\partial^2 w}{\partial r^2}+\frac{\partial^2 w}{\partial z^2}+\frac{1}{r}\frac{\partial w}{\partial r}\right), \tag{2.2}$$

where u is the radial velocity, w the axial velocity and p the fluid pressure. The continuity equation is given by

$$\frac{\partial u}{\partial r}+\frac{\partial w}{\partial z}+\frac{u}{r}=0 \tag{2.3}$$

and the kinematic boundary condition on the thread surface is

$$\frac{\partial a}{\partial t}+wa'=u \quad (r=a), \tag{2.4}$$

where primes denote $\partial/\partial z$.

The normal-stress condition on the thread surface is given by

$$p-\frac{2\mu}{(1+a'^2)}\left(\frac{\partial u}{\partial r}+a'^2\frac{\partial w}{\partial z}-a'\left(\frac{\partial w}{\partial r}+\frac{\partial u}{\partial z}\right)\right)=\sigma\kappa \quad (r=a), \tag{2.5}$$

where σ is the interfacial surface tension and

$$\kappa=\frac{1}{a(1+a'^2)^{1/2}}-\frac{a''}{(1+a'^2)^{3/2}} \tag{2.6}$$

is the interfacial curvature. The tangential-stress condition,

$$\frac{\mu}{(1+a'^2)^{1/2}}\left[\left(\frac{\partial w}{\partial r}+\frac{\partial u}{\partial z}\right)(1-a'^2)+2a'\left(\frac{\partial u}{\partial r}-\frac{\partial w}{\partial z}\right)\right]=\frac{\partial \sigma}{\partial z} \quad (r=a), \tag{2.7}$$

describes a balance of the viscous stress at the thread surface with the surface-tension gradients created by the transport of surfactant.

In addition to equations (2.1)–(2.7), we require a transport equation for the surfactant concentration Γ and an equation of state $\sigma(\Gamma)$. The effects of surfactant are twofold: first, it changes the magnitude of the surface tension, resulting in changes to the capillary pressure that drives the instability; secondly, a non-uniform surfactant distribution creates surface-tension gradients which result in surface shear stresses.

The changes in concentration of insoluble surfactant on a deforming liquid–gas interface are governed by

$$\frac{\partial \Gamma}{\partial t} = -\nabla_s \cdot (\Gamma \boldsymbol{u}_s) - \Gamma (\nabla_s \cdot \boldsymbol{n})(\boldsymbol{u} \cdot \boldsymbol{n}) \tag{2.8}$$

(Stone 1990), where $\Gamma(z,t)$ is the mass of surfactant per unit interfacial area, $\nabla_s = (\boldsymbol{I} - \boldsymbol{nn}) \cdot \nabla$ is the surface gradient operator, $\boldsymbol{u}_s = (\boldsymbol{I} - \boldsymbol{nn}) \cdot \boldsymbol{u}$ is the velocity along the surface and $\boldsymbol{n}$ is the unit normal to the interface; thus $\nabla_s \cdot \boldsymbol{n} = \kappa$. We have neglected surface diffusion of surfactant in (2.8) since chemical diffusivities are generally small. For example, if surfactant with typical diffusivity 10^{-10}–$10^{-9}\,\mathrm{mm^2\,s^{-1}}$ (Tricot 1997) were added to the liquid-bridge experiments of Zhang, Padgett & Basaran (1996), which had typical velocities greater than $1\,\mathrm{mm\,s^{-1}}$ and a lengthscale of order 1 mm, then the Péclet number would be at least 10^3–10^4. (On much smaller scales surface diffusion would result in a more uniform surfactant distribution (Hansen *et al.* 1999; Ambravaneswaran & Basaran 1999; Kwak & Pozrikidis 2001), countering convective effects; on very small scales or for very large diffusivities surfactant simply lowers the magnitude of a constant surface tension.)

We consider perturbations in surfactant concentration about an initially uniform concentration Γ_0 corresponding to a uniform surface tension σ_0 on the undisturbed thread. In the linear analysis, it is sufficient to use a linearized surface-tension equation of state

$$\sigma = \sigma_0 - E\left(\frac{\Gamma}{\Gamma_0} - 1\right), \tag{2.9}$$

where

$$E = -\Gamma_0 \left.\frac{\mathrm{d}\sigma}{\mathrm{d}\Gamma}\right|_{\Gamma_0} \tag{2.10}$$

is the Gibbs elasticity. In nonlinear calculations, it would be better to use the Frumkin equation of state in the form

$$\sigma = \sigma_0 + RT\Gamma_\infty \ln\left(\frac{\Gamma_\infty - \Gamma}{\Gamma_\infty - \Gamma_0}\right), \tag{2.11}$$

where R is the gas constant, T is temperature and Γ_∞ is the experimentally determined maximum adsorption density, which is a reasonable approximation for many surfactants (Tricot 1997).

3. Linear stability

3.1. *Characteristic equation*

We use linear stability theory to investigate the behaviour of a small disturbance to an initially uniform, stationary, unbounded liquid thread uniformly coated with insoluble surfactant. We assume that all variables are perturbed only slightly from their stationary values and that the perturbations have the normal-mode form

$$(u, w, \delta p, \delta a, \delta\sigma, \delta\Gamma) = (\hat{u}(r), \hat{w}(r), \widehat{\delta p}(r), \widehat{\delta a}, \widehat{\delta\sigma}, \widehat{\delta\Gamma}) \exp(\mathrm{i}kz + \alpha t), \tag{3.1}$$

where k is the wavenumber, α the growth rate of the disturbance and δ denotes the perturbation from a non-zero initial value.

In a similar manner to Tomotika (1935), we linearize the system (2.1)–(2.8) and solve the linear system to determine the evolution of the perturbed quantities. In this

way, we deduce the characteristic equation

$$\alpha^2\mathrm{F}(kR) + \frac{2k^2\alpha\mu}{\rho}(2\mathrm{F}(kR)-1) + \frac{4\mu^2k^4}{\rho^2}(\mathrm{F}(kR)-\mathrm{F}(\tilde{k}R)) - \frac{k^2\sigma_0}{\rho R}(1-k^2R^2) + \frac{k^4\mu E}{\alpha\rho^2 R}\left(2-\frac{\sigma_0}{\alpha R\mu}(1-k^2R^2)\right)(\mathrm{F}(\tilde{k}R)-\mathrm{F}(kR)) + \frac{Ek^2}{\rho R}(1+\mathrm{F}(kR)[\mathrm{F}(\tilde{k}R)-2]) = 0, \tag{3.2}$$

where R is the unperturbed radius of the thread,

$$\tilde{k}^2 = k^2 + \frac{\rho}{\mu}\alpha \quad \text{and} \quad \mathrm{F}(x) = \frac{xI_0(x)}{I_1(x)}. \tag{3.3}$$

This characteristic equation may also be deduced by taking the limit of equation (4.43) of Hansen *et al.* (1999) for a thread of density and viscosity very much greater than its surroundings and that is coated with surfactant having zero bulk and surface diffusivities. It corrects two mistakes in equation (84) of Whitaker (1976). Here, we focus on analytic exploration of limits and transitions in (3.2) in order to gain understanding of the dominant physical balances.

3.2. *Non-dimensionalization*

There are various ways to non-dimensionalize (3.2) and it is worth considering the options. Different ratios of the main dynamical effects define three commonly used dimensionless parameters: the Weber number $We = \rho RU^2/\sigma_0$, where U is the velocity scale, describes the ratio of inertial forces to surface-tension forces; the capillary number $Ca = \mu U/\sigma_0$ describes the ratio of viscous to surface-tension forces; and the Reynolds number $Re = \rho UR/\mu$ describes the ratio of inertial to viscous forces. Each of these parameters requires an estimate of the velocity scale U, but the appropriate choice depends upon the dominant force balance. In the viscous limit, when viscous and surface-tension forces are comparable and inertia is not important, (2.1) implies that $U \sim \sigma_0/\mu$. The appropriate definition for the Reynolds number is then $Re = \rho\sigma_0 R/\mu^2$, and in this regime $Ca = O(1)$ while $We \ll 1$. In the inviscid limit, however, a balance of inertial and surface-tension forces gives $U \sim \sigma_0/(\rho R)^{1/2}$. The appropriate definition for the Reynolds number is now $Re = (\rho\sigma_0 R/\mu^2)^{1/2}$, and in this regime $We = O(1)$ while $Ca \ll 1$.

Since the velocity scale depends upon the relevant force balance, results are sometimes expressed in terms of the Ohnesorge number $Oh = \mu/(\rho\sigma_0 R)^{1/2}$, which depends only on the fluid properties and geometry. Other scalings can be recovered from the relationships $Oh^2 = We/Re^2 = Ca/Re$. Since these numbers are based on σ_0, the mean reduction in interfacial tension by the surfactant is incorporated into the scaling. This is appropriate since we are primarily concerned with flow-induced variations in surfactant concentration. Typical values of the Ohnesorge number are $Oh \approx 10^{-4}$ for a water thread of diameter 1 mm in air and $Oh \approx 10^2$ for a similar glycerol thread.

We non-dimensionalize the wavenumber k by the unperturbed radius R, and the growth rate α by the capillary timescale $\mu R/\sigma_0$ to express the characteristic equation (3.2) in the non-dimensional form

$$\mathscr{R}\alpha^2\mathrm{F}(k) + 2k^2\alpha(2\mathrm{F}(k)-1) + \frac{4k^4}{\mathscr{R}}(\mathrm{F}(k)-\mathrm{F}(\tilde{k})) - k^2(1-k^2) + \frac{k^4\beta}{\mathscr{R}\alpha}\left(2-\frac{1-k^2}{\alpha}\right)(\mathrm{F}(\tilde{k})-\mathrm{F}(k)) + \beta k^2(1+\mathrm{F}(k)[\mathrm{F}(\tilde{k})-2]) = 0, \tag{3.4}$$

where

$$\tilde{k}^2 = k^2 + \mathscr{R}\alpha, \tag{3.5}$$

$$\mathscr{R} = Oh^{-2} = \frac{\rho\sigma_0 R}{\mu^2}, \tag{3.6}$$

and both k and α are now dimensionless. The parameter $\mathscr{R}$ is equal to Re for $\mathscr{R} \ll 1$ and Re^2 for $\mathscr{R} \gg 1$. The parameter

$$\beta = -\left.\frac{\Gamma_0}{\sigma_0}\frac{\mathrm{d}\sigma}{\mathrm{d}\Gamma}\right|_{\Gamma_0} = \frac{E}{\sigma_0} \tag{3.7}$$

is a dimensionless measure of the strength of the surfactant with $0 \leqslant \beta < \infty$.

When $\beta = 0$, (3.4) reduces to Rayleigh's well-known characteristic equation for a viscous thread surrounded by a fluid of negligible viscosity (Rayleigh 1892). An infinitesimal perturbation, of wavelength $2\pi/k$, to the free surface of the thread grows exponentially provided k lies in the band $0 \leqslant |k| < 1$ for which the destabilizing perturbation to the azimuthal curvature exceeds the stabilizing perturbation to the axial curvature. Moreover, there is a unique wavenumber k_m in this band which gives a maximum growth rate α_m.

3.3. *Long-wave expansion*

The characteristic equation (3.4) is complicated because $\tilde{k}$ is a function of α, so that α is contained in the arguments of some of the Bessel functions. In order to gain some analytical insight, we consider a simpler form of the equation valid in the long-wave limit $|k| \ll 1$. As shown below, this situation is particularly relevant to viscous threads for which $k_m \ll 1$.

Subject to *a posteriori* confirmation, we assume that $\mathscr{R}\alpha \ll 1$ as $k \to 0$. For small arguments, series expansion of the Bessel functions gives $\mathrm{F}(x) = 2(1 + x^2/8 - x^4/48) + O(x^6)$. We can thus expand (3.4) for $|k| \ll 1$ as

$$\frac{2\mathscr{R}\alpha^2}{k^2} - 1 + 6\alpha + \beta\left(1 + \frac{\mathscr{R}\alpha}{2}\right) + k^2 + \beta k^2\left(-\frac{1}{4\alpha} + 1 + \frac{\mathscr{R}}{24}\right) + \frac{\beta k^4}{3\alpha} = O(k^4, k^2\alpha, \alpha^2). \tag{3.8}$$

In the simple case $\beta = 0$ we deduce from a balance of the first two terms that $\alpha \sim k$ for small k. If we assume that $\alpha \sim k$ for $\beta > 0$, (3.4) is solved to leading order by

$$\alpha^2 = \frac{k^2}{2\mathscr{R}}(1 - \beta). \tag{3.9}$$

The requirement that $\mathscr{R}\alpha \ll 1$ as $k \to 0$ thus implies that $k \ll \mathscr{R}^{-1/2}$ and that there is a non-uniformity with the inviscid limit $\mathscr{R} \to \infty$. (Non-uniformities between various limits in k and $\mathscr{R}$ occur throughout the remainder of § 3. The domains of validity are shown schematically in figure 1 to allow the relationship between the results to be seen more easily.)

Clearly, some transition also occurs at $\beta = 1$, suggesting that (3.9) is only applicable for $\beta < 1$. In order to investigate $\beta > 1$, we first consider the limit $\beta \gg 1$. For $\beta \to \infty$, the long-wave limiting form of (3.4) is given by

$$1 - \frac{k^2}{4\alpha} + \frac{\mathscr{R}\alpha}{2} + k^2\left(1 + \frac{\mathscr{R}}{24}\right) + \frac{k^4}{3\alpha} = 0, \tag{3.10}$$

and from a balance of the first two terms $\alpha \sim k^2$ in this limit. If we assume that

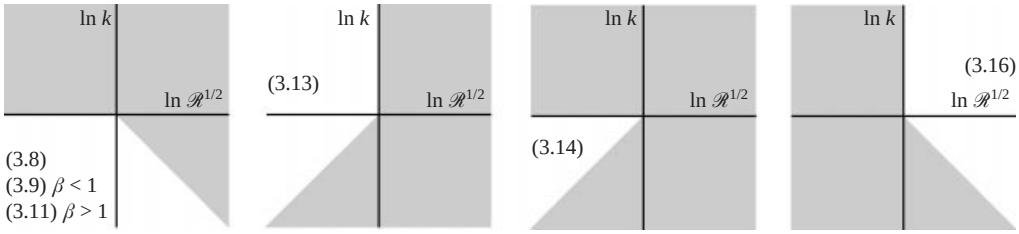

FIGURE 1. Schematic representation of the domains of validity for the various asymptotic expansions in § 3 of the characteristic equation (3.4). For example, (3.8), (3.9) and (3.11) all require both $k \ll 1$ and $k \ll \mathscr{R}^{-1/2}$.

$\alpha \sim k^2$, (3.4) is given to leading order by

$$\alpha = \frac{k^2}{4}\frac{\beta}{\beta - 1}, \tag{3.11}$$

which is only valid for $\beta > 1$.

The change in leading-order behaviour at $\beta = 1$ is a result of a transition from extension-dominated to shear-dominated flow as β increases through 1, and will be discussed further in § 4.4. The difference between (3.9) and (3.11) shows a non-uniformity of the limits $\beta \to 1$ and $k \to 0$, which is resolved by noting that (3.9) is valid only for $k \ll (1-\beta)^{3/2}\mathscr{R}^{-1/2}$ while (3.11) requires $k \ll (\beta - 1)^{3/2}\mathscr{R}^{-1/2}$ as $\beta \to 1$. (For the special case $\beta \equiv 1$ between (3.9) and (3.11) the long-wave limit gives an intermediate form $\alpha = (k^4/8\mathscr{R})^{1/3}$.)

Equations (3.9) and (3.11) also differ in their dependence on $\mathscr{R}$, which motivates examination of the limits of inviscid and very viscous threads and the corresponding long-wave expansions.

3.4. *Viscous thread*

In the viscous limit, $\mathscr{R} \to 0$, the effects of inertia can be neglected relative to viscosity. In this limit, (3.5) can be approximated by

$$\tilde{k} \approx k + \frac{\mathscr{R}\alpha}{2k}, \tag{3.12}$$

and we take a Taylor series of $\mathrm{F}(\tilde{k})$ about k to find that (3.4) becomes

$$2\alpha(\mathrm{F}(k)^2 - 1 - k^2) - (1 - k^2) + \beta(1 + k^2) - \beta\frac{(1-k^2)}{2\alpha}(k^2 + 2\mathrm{F}(k) - \mathrm{F}(k)^2) = 0 \tag{3.13}$$

as $\mathscr{R} \to 0$. This equation is valid for $k^2 \gg \mathscr{R}$, but fails if $k^2 \to 0$ faster than $\mathscr{R} \to 0$.

When $\beta = 0$ equation (3.13) coincides with Rayleigh's surfactant-free result (Rayleigh 1892). In particular, the growth rate is maximal when $k = 0$, so that the most unstable perturbation has infinite wavelength, as shown in figure 2(*a*). However, if the small inertia terms are retained for $\mathscr{R} \ll 1$, the most unstable wavenumber is non-zero as shown in figure 2(*b*).

The scaling of the long-wave cut-off provided by a small amount of inertia has not, to our knowledge, been analysed directly from the full equations. Figure 3 shows $\alpha_m(\mathscr{R})$ and $k_m(\mathscr{R})$ as calculated from the full characteristic equation (3.4) with $\beta = 0$. The asymptotic behaviour in the viscous limit $\mathscr{R} \to 0$ suggests that $\alpha_m = O(1)$ and $k_m \propto \mathscr{R}^{1/4}$. This is confirmed by expansion of (3.4) with $k \ll 1$, $\mathscr{R} \ll 1$ and $\alpha = O(1)$,

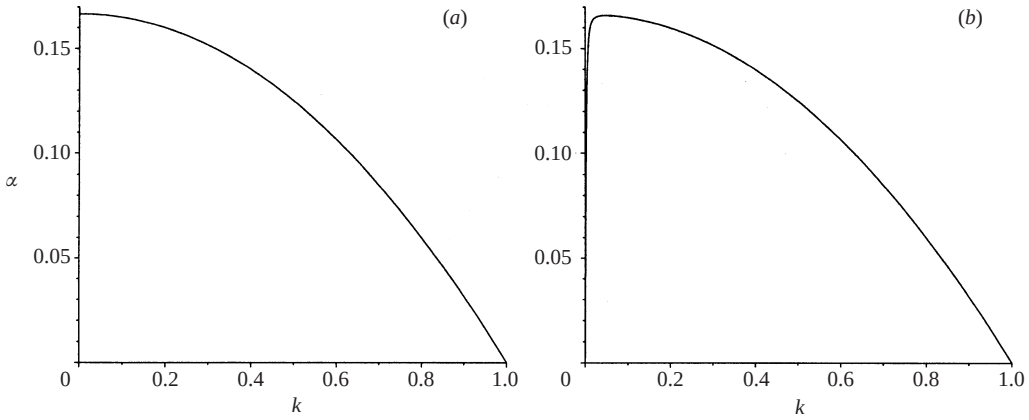

FIGURE 2. Growth rate α as a function of wavenumber k for a very viscous thread with no surfactant ($\beta = 0$) and (*a*) $\mathscr{R} = 0$ (zero inertia), (*b*) $\mathscr{R} = 10^{-4}$ (small inertia). Inertia provides a long-wave cut-off.

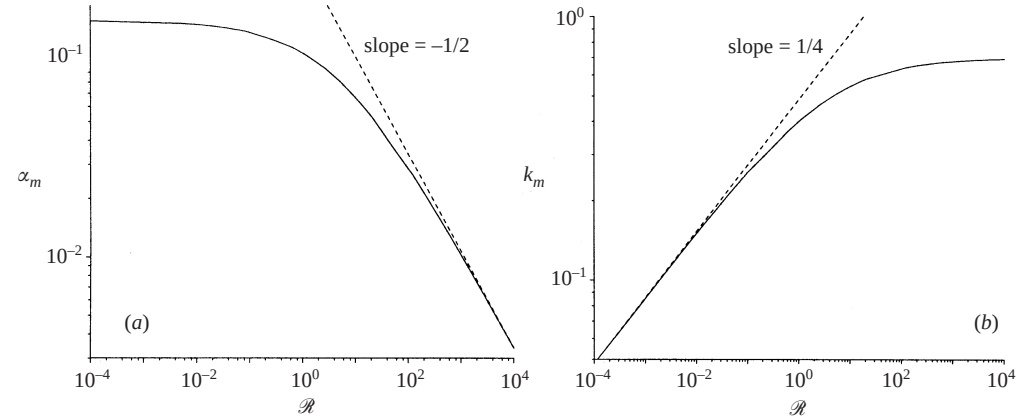

FIGURE 3. (*a*) α_m and (*b*) k_m as functions of $\mathscr{R}$ (solid curves) for a surfactant-free thread ($\beta = 0$). The asymptotes (dashed) show that $\alpha_m \sim \mathscr{R}^{-1/2}$ in the inviscid regime and $k_m \sim \mathscr{R}^{1/4}$ in the viscous regime.

to obtain

$$\frac{2\mathscr{R}\alpha^2}{k^2} + 6\alpha - 1 + k^2 + \beta\left(1 + k^2 - \frac{k^2}{4\alpha}\right) + O(k^4, \mathscr{R}) = 0. \tag{3.14}$$

When $\beta = 0$, the second and third terms balance at leading order to give $\alpha \sim \frac{1}{6}$; the weakly maximal growth rate is found by optimizing the first and fourth terms to obtain $k_m \sim (\mathscr{R}/18)^{1/4}$ and $\alpha_m \sim \frac{1}{6} - (\mathscr{R}/2)^{1/2}$. The optimized terms correspond to inertia and the axial curvature; corrections to the leading-order extensional viscous stresses are, somewhat surprisingly, higher order in the linear problem.

3.5. *Inviscid thread*

In the inviscid limit, $\mathscr{R} \to \infty$, viscosity can be neglected relative to inertia. In this limit (3.5) can be approximated by

$$\tilde{k} \approx (\mathscr{R}\alpha)^{1/2}\left(1 + \frac{k^2}{2\mathscr{R}\alpha}\right). \tag{3.15}$$

We take a Taylor series of $\mathrm{F}(\tilde{k})$ about $(\mathscr{R}\alpha)^{1/2}$ and use asymptotic expansions of the modified Bessel functions for large arguments (Abramovich & Stegun 1965) to find that $\mathrm{F}(x) \sim x$ for $x \gg 1$. Hence $\mathrm{F}(\tilde{k}) \sim (\mathscr{R}\alpha)^{1/2}$ as $\mathscr{R} \to \infty$, and (3.4) becomes

$$\alpha^2 = \frac{k^2(1-k^2)}{\mathscr{R}\mathrm{F}(k)}. \tag{3.16}$$

The scaling $\alpha_m \sim \mathscr{R}^{-1/2}$ as $\mathscr{R} \to \infty$ also follows by dimensional analysis and independence of μ and is apparent in figure 3(*a*). Equation (3.16) is valid for all β when $\mathscr{R} \gg 1$ and, since it is independent of β, it agrees with Rayleigh's result for a surfactant-free inviscid thread (Rayleigh 1879, 1892). Thus, in the inviscid limit, surfactant plays no role other than to reduce the mean value of the surface tension, as noted also by Whitaker (1976) and Hansen *et al.* (1999). The reason is two-fold. First, surfactant gradients cannot persist on the surface of an inviscid thread because any surface-tension gradients would drive a boundary-layer flow uninhibited by viscous forces which would rapidly restore a uniform surfactant distribution. Second, any tangential stresses in such a boundary-layer flow would not be communicated to the interior of an inviscid thread.

The long-wave limit of (3.16) gives $\alpha^2 = k^2/2\mathscr{R}$ at leading order independent of β, whereas the inviscid limit with $k \ll \mathscr{R}^{-1/2} \ll 1$ of the long-wave expansion (3.8) is (3.9). The non-commutation of these limits is due to the fact that the long-wave limit averages surfactant stresses over the cross-section, whereas the inviscid limit confines them to surface boundary layers; the boundary $k \sim \mathscr{R}^{-1/2}$ corresponds to the lengthscale required for viscous diffusion of surface stresses into the interior.

3.6. *The effects of surfactant*

3.6.1. *Large tangential stresses* $\beta \to \infty$

The parameter β represents the strength of the effect of variations in surface tension $(\mathrm{d}\sigma/\mathrm{d}\Gamma)\delta\Gamma$ made dimensionless with respect to the mean surface tension σ_0. As $\beta \to \infty$, the limiting form of (3.4) is

$$\mathscr{R}\alpha^2(1 + \mathrm{F}(k)\{\mathrm{F}(\tilde{k}) - 2\}) + 2k^2\alpha\{\mathrm{F}(\tilde{k}) - \mathrm{F}(k)\} - k^2(1-k^2)\{\mathrm{F}(\tilde{k}) - \mathrm{F}(k)\} = 0, \tag{3.17}$$

which gives a non-zero growth rate independent of β.

It is worth outlining how (3.17) can also be derived by using the intuitive notion that strong surfactant effects tend to immobilize an interface, since two points need clarification. First, as $\beta \to \infty$, the surface velocities must be such that Γ remains approximately uniform since significant gradients in Γ would drive a strong restoring flow. While this simply requires a zero tangential velocity on a non-deforming interface (e.g. rigidification near the rear stagnation point of a rising contaminated bubble, or the factor of 4 decrease in flux from rigid-free to rigid-rigid boundary conditions in film flow), for a deforming interface (2.8) yields the condition

$$\frac{\partial w}{\partial z} + \frac{u}{a} = 0 \quad (r = a) \tag{3.18}$$

(cf. (5.18) in Hansen *et al.* 1999) with corrections at $O(\beta^{-1})$. Thus the tangential flow is non-zero but must balance the radial dilatation. Second, the perturbation from uniform surface tension is not negligible, as stated for example by Hansen *et al.* (1999), but rather is an $O(1)$ quantity derived from $O(\beta^{-1})$ variations in Γ multiplied by an $O(\beta)$ dependence of σ on these variations. The characteristic equation for $\beta \to \infty$ can thus be obtained directly by replacing (2.8) by (3.18) in the linearized

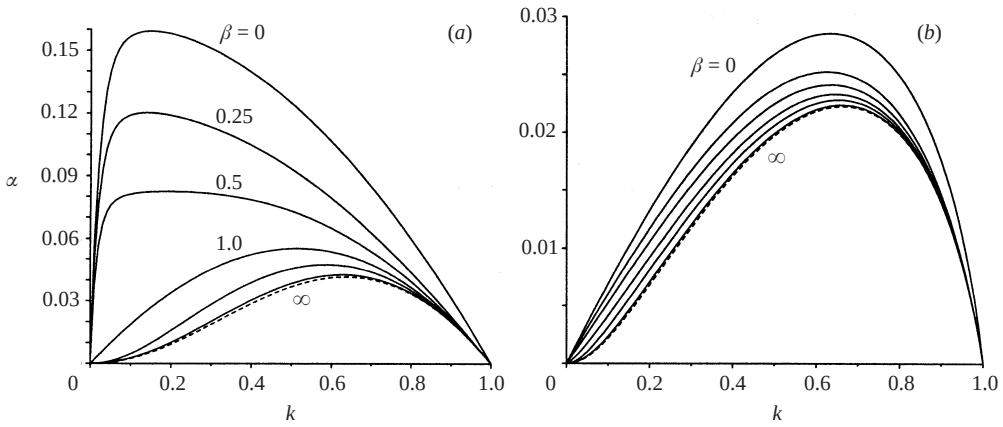

FIGURE 4. Growth rate α as a function of wavenumber k for $\beta = 0$ (top curves), 0.25, 0.5, 1, 2, 10. The limit $\beta \to \infty$ (dashed) is given by (3.17). (*a*) $\mathscr{R} = 0.01$ (*b*) $\mathscr{R} = 100$. Surfactant has a much greater effect on a viscous thread. The effects of surfactant disappear as $\mathscr{R} \to \infty$ (3.16).

perturbation equations. Equation (3.18) functions as a tangential-stress condition, and (2.7) now enables the surface-tension perturbation $\delta\sigma$ to be calculated from u and w. Similar reasoning could be applied to other flow geometries.

3.6.2. *Surfactant concentrations* $0 < \beta < \infty$

Figure 4 shows the effect of the surface-tension-gradient parameter β on $\alpha(k)$ as computed from (3.4). In the presence of surfactant, the growth rate α still has a maximum α_m for some wavenumber k_m in the range $0 < k < 1$. The most obvious result is that surfactant reduces the growth rate of disturbances to the thread. The limiting form (3.17) for $\beta \to \infty$ (dashed curves) thus provides a lower bound for the growth rate for each $\mathscr{R}$.

The influence of surfactant is much less in the inviscid regime (large $\mathscr{R}$) than in the viscous regime (small $\mathscr{R}$), and the dominant wavenumber changes little for $\mathscr{R} = 100$ over the whole range $0 \leqslant \beta < \infty$. For $\mathscr{R} = 0.01$ the tangential stresses caused by surface-tension gradients significantly modify the flow and cause a dramatic shift to shorter wavelengths as β increases beyond 0.5. The related change in long-wave scaling noted earlier, from $\alpha \sim k$ (3.9) to $\alpha \sim k^2$ (3.11) as β increases through 1, is clearly seen in figure 5.

The effects of surfactant on the dominant long-wave instability for the viscous limit $\mathscr{R} \ll 1$ can be found from (3.14). The leading-order terms for $k \ll 1$ with $\alpha = O(1)$ give $\alpha \sim (1 - \beta)/6$. Looking for a long-wave inertial cut-off for $0 < \mathscr{R} \ll 1$ results in

$$k_m^4 = \frac{\mathscr{R}(1-\beta)^3}{18(\beta+2)(\frac{1}{2}-\beta)} \quad (\beta < \tfrac{1}{2}) \tag{3.19}$$

so that $k_m = O(\mathscr{R}^{1/4})$ again provided that $\beta < \frac{1}{2}$. The divergence as $\beta \nearrow \frac{1}{2}$ suggests that surfactant is taking over the long-wave cut-off from inertia.

Figure 6(*a*) shows $\alpha(k)$ for $\mathscr{R} = 0$, as described by (3.13). Small values of β give a maximum growth rate at $k = 0$, but large values give a maximum growth rate at a finite wavelength. If we let $\mathscr{R} \to 0$ and rewrite (3.14) as

$$\alpha = \frac{1-\beta}{6} + A\frac{k^2}{6} + O(k^4), \tag{3.20}$$

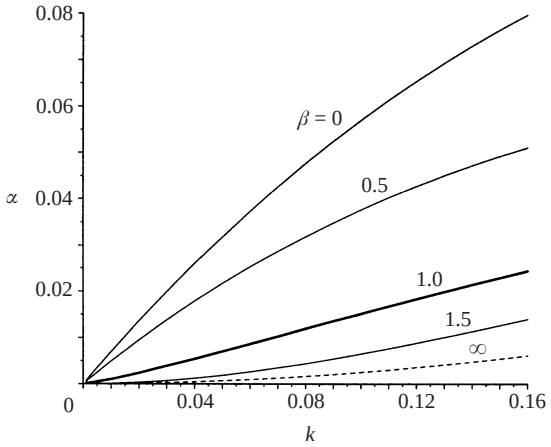

FIGURE 5. Growth rate $\alpha(k)$ for $k \ll 1$ with $\mathscr{R} = 1$ and $\beta = 0$ (top curve), 0.5, 1, 1.5 and ∞ (dashed). For $k \ll 1$ there is a transition from $\alpha \sim k$ for $\beta < 1$ through $\alpha \sim k^{4/3}$ for $\beta = 1$ to $\alpha \sim k^2$ for $\beta > 1$.

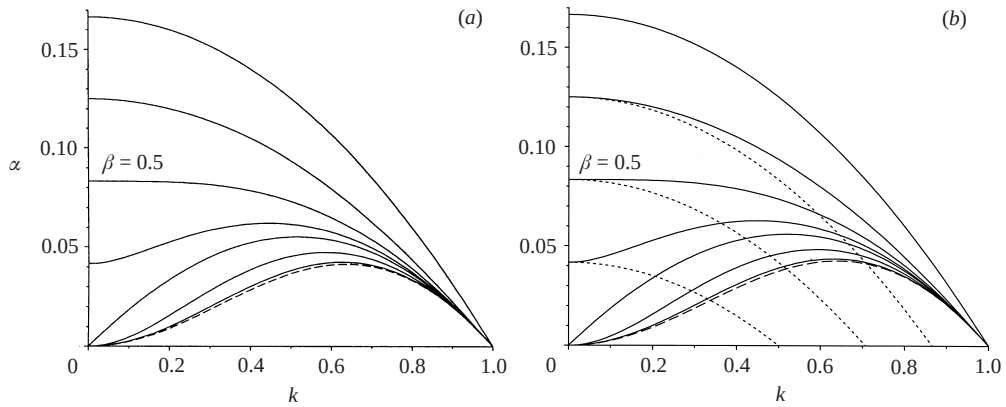

FIGURE 6. (*a*) Variation of the growth rate $\alpha(k)$ from (3.13) for a very viscous thread ($\mathscr{R} = 0$) for $\beta = 0$ (top curve), 0.25, 0.5, 0.75, 1, 2 and 10. In the limit $\beta \to \infty$ (dashed) $k_m \to 0.6361$ and $\alpha_m \to 0.0415$. (*b*) The growth rate (4.15) of the $O(\epsilon^4)$ one-dimensional model (4.12)–(4.14) (solid) is virtually identical to that of the full axisymmetric equations. In the limit $\beta \to \infty$ (dashed) $k_m \to 0.6409$ and $\alpha_m \to 0.0426$. The growth rate (4.18) of the $O(\epsilon^2)$ model (4.16)–(4.14) (dotted for $\beta = 0.25, 0.5, 0.75$) is the same for $\beta = 0$, but fails to show the important changes in behaviour at $\beta = \frac{1}{2}$ and $\beta = 1$.

where

$$A = \frac{\beta}{4\alpha} - (1 + \beta), \tag{3.21}$$

it is clear that this change in behaviour occurs when $A = 0$. We substitute $\alpha_m = (1 - \beta)/6$ into (3.21) to find that $k_m > 0$ for $\mathscr{R} = 0$ if $\beta > \frac{1}{2}$. Palierne & Lequeux (1991) found a similar feature for a critical value of an interfacial 'dilatational modulus.' However, they did not determine the form of the modulus, which requires coupling the surfactant evolution equation to the equations of motion.

Prediction of the finite dominant wavelength for a very viscous thread is an important case to consider. We conclude from the above that if $\beta < \frac{1}{2}$ then inertia provides a long-wave cut-off and $k_m = O(\mathscr{R}^{1/4})$ whereas if $\beta > \frac{1}{2}$ then surfactant provides a long-wave cut-off and $k_m = O(1)$. Inclusion of an external fluid with small

viscosity $\lambda\mu$ also provides a mechanism for long-wave cut-off (Tomotika 1935) with $k_m = O(\lambda^{1/4})$ and in this case the dominant mechanism is given by the largest of $\beta - \frac{1}{2}$, $\mathscr{R}^{1/4}$ and $\lambda^{1/4}$.

4. One-dimensional nonlinear approximations

The dynamics of the free surface close to breakup of the thread cannot be described by linear theory and a fundamentally different approach is required for the fully nonlinear regime. The full three-dimensional Navier–Stokes equations for the dynamics are computationally expensive, even in the axisymmetric limit. However, the dynamics are known to be dominated by long-wave behaviour both in the linearized viscous limit from § 3.4 and close to breakup when there is no surfactant (Eggers 1993). The aim of this section is to develop a one-dimensional long-wave approximation that describes the effects of surfactant into the nonlinear regime. Formal procedures for systematic derivation of a hierarchy of long-wave approximations for the case of no surfactant are described in Eggers & Dupont (1994), Garcia & Castellanos (1994), Bechtel, Carlson & Forest (1995) and Eggers (1997). Here we shall proceed less formally and more directly to an approximation of sufficient accuracy to capture the variation of the linearly most unstable wavelength for $\beta < \frac{1}{2}$. This approximation, analogous to the averaged parabolic model of Garcia & Castellanos (1994), necessarily involves higher-order corrections to the viscous and inertia terms than are needed for $\beta = 0$.

4.1. *Derivation*

In a long-wave approximation we assume that the typical axial lengthscale of variation is much greater than the typical radial scale so that, for example, a' and $a\,\partial/\partial z$ are $O(\epsilon)$, where $\epsilon \ll 1$. If radial variations are small then u, w and p are well-represented by the first few terms in their radial power series, and we write

$$w(r,z,t) = \bar{w}(z,t) + \left(\frac{r^2}{a^2} - \frac{1}{2}\right) w_1(z,t), \tag{4.1}$$

$$p(r,z,t) = \overline{p}(z,t) + \left(\frac{r^2}{a^2} - \frac{1}{2}\right) p_1(z,t), \tag{4.2}$$

$$u(r,z,t) = -\tfrac{1}{2} r\bar{w}' - \tfrac{1}{4} r^3 \left(\frac{w_1}{a^2}\right)' + \tfrac{1}{4} r w_1'. \tag{4.3}$$

Here $\bar{w}$ and $\overline{p}$ denote the (exact) cross-sectional averages of w and p, and w_1 and p_1 denote the amplitudes of the small average-free quadratic correction. We shall find that $w_1/\bar{w}$ and $p_1/\overline{p}$ are $O(\epsilon^2)$ if $\beta < 1$; the omitted quartic corrections are $O(\epsilon^4)$. The form of u is obtained from that of w by mass conservation.

The advantage of expanding about the cross-sectional average is that the governing equations (2.1)–(2.7) can be rewritten in exact conservation form as

$$\frac{\partial}{\partial t}(a^2) + \frac{\partial}{\partial z}(a^2\bar{w}) = 0, \tag{4.4}$$

$$\frac{\partial}{\partial t}(\rho a^2\bar{w}) + \frac{\partial}{\partial z}(\rho a^2\overline{w^2}) = \frac{\partial}{\partial z}\left(-a^2\overline{p} + 2\mu a^2\overline{\frac{\partial w}{\partial z}} + \frac{2a\sigma}{(1+a'^2)^{1/2}}\right). \tag{4.5}$$

The dimensionless form is obtained by replacing ρ by $\mathscr{R}$ and μ by 1. Since $\overline{w^2} =$

$\bar{w}^2 + O(w_1^2)$ and $\partial(a^2\bar{w})/\partial z = a^2\overline{\partial w/\partial z} + 2aa'w(a)$, a little manipulation produces

$$\mathscr{R}a^2\left(\frac{\partial \bar{w}}{\partial t} + \bar{w}\frac{\partial \bar{w}}{\partial z}\right) = \frac{\partial}{\partial z}\left(-a^2\bar{p} + 2a^2\frac{\partial \bar{w}}{\partial z} - 2aa'w_1 + \frac{2a\sigma}{(1+a'^2)^{1/2}}\right) \tag{4.6}$$

with $O(\epsilon^4)$ relative errors.

Substitution of (4.1) and (4.3) into the tangential-stress boundary condition (2.7) yields

$$w_1 = \tfrac{3}{2}aa'\bar{w}' + \tfrac{1}{4}a^2\bar{w}'' + \tfrac{1}{2}a\sigma' \tag{4.7}$$

with $O(\epsilon^2)$ relative errors. If $2(a^2\bar{w}')'$ and $2(a\sigma)'$ are both leading-order terms in (4.6) then $a\sigma' = O(a^2\bar{w}'')$, and (4.7) confirms that $w_1/\bar{w}$ is $O(\epsilon^2)$. The normal-stress boundary condition (2.5) is approximated by

$$\bar{p} + \tfrac{1}{2}p_1 = \sigma\kappa + 2\left\{\frac{\partial u}{\partial r} - a'\left(\frac{\partial w}{\partial r} + \frac{\partial u}{\partial z}\right) + a'^2\left(\frac{\partial w}{\partial z} - \frac{\partial u}{\partial r}\right)\right\} \tag{4.8}$$

with $O(\epsilon^4)$ relative errors. Substitution of (4.1) and (4.3) yields

$$\bar{p} = \sigma\kappa - \bar{w}' - w_1' - a'w_1/a + 3a'^2\bar{w}' + aa'\bar{w}'' - \tfrac{1}{2}p_1 \tag{4.9}$$

with the same errors. Finally, substitution of (4.1)–(4.3) into the radial momentum equation (2.1) yields

$$\mathscr{R}(-\tfrac{1}{2}\dot{\bar{w}}' + \tfrac{1}{4}\bar{w}'^2 - \tfrac{1}{2}\bar{w}\,\bar{w}'') = -2p_1/a^2 - \tfrac{1}{2}\bar{w}''' - 2(w_1/a^2)' \tag{4.10}$$

with $O(\epsilon^2)$ relative errors, where an overdot denotes $\partial/\partial t$. Equations (4.9) and (4.10) confirm the relative magnitudes of $\bar{p}$ and p_1. We now use (4.7)–(4.10) to eliminate $\bar{p}$, w_1 and p_1 from (4.6), and apply the identity

$$\frac{\partial}{\partial z}\left(\frac{2a}{(1+a'^2)^{1/2}}\right) = \kappa\frac{\partial a^2}{\partial z}. \tag{4.11}$$

The resultant evolution equation for $\bar{w}$ is

$$\begin{aligned}\mathscr{R}a^2\left(\dot{\bar{w}} + \bar{w}\,\bar{w}'\right) - \tfrac{1}{8}\mathscr{R}[a^4(\dot{\bar{w}}' - \tfrac{1}{2}\bar{w}'^2 + \bar{w}\,\bar{w}'')]' &= -a^2(\sigma\kappa)' + 2a\sigma'/(1+a'^2)^{1/2} \\ &\quad + \tfrac{1}{4}\left[a^2(a\sigma')'\right]' + 3[(a^2 + \tfrac{1}{4}a^3a'' - \tfrac{3}{4}a^2a'^2)\bar{w}']'\end{aligned} \tag{4.12}$$

accurate to relative error $O(\epsilon^4)$. The evolution equations for a and Γ are obtained from (4.4) and (2.8) as

$$\dot{a} + \bar{w}a' = -\tfrac{1}{2}a\bar{w}', \tag{4.13}$$

$$\dot{\Gamma} + [\Gamma(\bar{w} + \tfrac{1}{2}w_1)]' = \tfrac{1}{2}\Gamma\kappa(a\bar{w}' - a'w_1), \tag{4.14}$$

where w_1 can be eliminated from (4.14) using (4.7). Equations (4.12)–(4.14), together with the equation of state $\sigma(\Gamma)$, then form a closed one-dimensional model for the long-wave evolution.

4.2. *Linear behaviour*

The characteristic equation for linear disturbances to a uniform state in the one-dimensional model is

$$\frac{2\mathscr{R}\alpha^2}{k^2} - 1 + 6\alpha + \beta + \frac{\alpha\beta\mathscr{R}}{2} + \frac{\alpha^2\mathscr{R}}{4} + k^2\left(1 + \beta - \frac{\beta}{4\alpha} + \frac{\alpha\beta\mathscr{R}}{16}\right) + \frac{k^4\beta(\alpha+4)}{16\alpha} = 0. \tag{4.15}$$

This differs from the full characteristic equation (3.4) at $O(k^4, k^2\mathscr{R}, \mathscr{R}^2)$, which is as expected for $k = O(\epsilon)$ provided $\mathscr{R}\alpha = O(\epsilon^2)$. Crucially, the $O(k^2)$ terms are correct, and hence the most unstable wavelength in the one-dimensional model is given by (3.19) for $\beta < \frac{1}{2}$ and $\mathscr{R} \ll 1$. (If $\beta > \frac{1}{2}$ or $\mathscr{R} \geqslant O(1)$ there is no reason to expect long-wave behaviour to dominate the linear regime.)

From studies of thread without surfactant it would be tempting to use the simpler $O(\epsilon^2)$ long-wave model

$$\mathscr{R}a^2(\dot{\bar{w}} + \bar{w}\,\bar{w}') = -a^2(\sigma\kappa)' + 2a\sigma' + 3(a^2\bar{w}')', \tag{4.16}$$

$$\dot{\Gamma} + (\Gamma\,\bar{w})' = \tfrac{1}{2}\Gamma\,\bar{w}', \tag{4.17}$$

together with (4.13). However, this gives the characteristic equation

$$\frac{2\mathscr{R}\alpha^2}{k^2} - 1 + 6\alpha + \beta + k^2 = 0, \tag{4.18}$$

which differs at $O(k^2)$ from the long-wave expansion (3.8) and fails to show the long-wave cut-off provided by surfactant for $\beta > \frac{1}{2}$. Somewhat fortunately, it does give the most unstable wavelength for $\beta = 0$ since the sole $O(k^2)$ linear term is captured by use of the full curvature κ, while the comparable corrections $\frac{3}{4}a^3a'' - \frac{9}{4}a^2a'^2$ to the extensional viscosity in (4.12) only appear in the nonlinear problem. Comparison of the characteristic equations (4.15) and (4.18) in figure 6(*b*) shows that the $O(\epsilon^4)$ model reproduces all the features of the full characteristic equation with surprising accuracy, while the $O(\epsilon^2)$ model can be misleading unless β is small.

4.3. *Scaling analysis near breakup*

Very close in time and space to the point where a fluid thread or drop breaks into two drops, there is no externally imposed lengthscale and the evolution of the free-surface shape is self-similar and independent of initial conditions. Various dynamical regimes in the absence of surfactant have been analysed, as reviewed by Lister *et al.* (1997), and the corresponding similarity solutions derived. In particular, we note that, in the presence of a non-zero external viscosity, however small, the eventual asymptotic balance is between internal and external viscous stresses and surface tension, with inertia being negligible (Lister & Stone 1998).

If there is no external viscosity and no surfactant ($\beta = 0$) then the asymptotic behaviour near breakup is described by (4.13) and (4.16) with σ constant, for which self-similar solutions have been found by Eggers (1993) and Brenner, Lister & Stone (1996). These solutions balance inertial, viscous and surface-tension terms in (4.16) so that

$$z \sim \tau^{1/2}, \quad w \sim \tau^{-1/2} \quad \text{and} \quad a \sim \tau, \tag{4.19}$$

where τ is the time remaining until the thread pinches off at $z = 0$. When $\beta \neq 0$, we can use scaling analysis to argue that surfactant has little effect on the self-similar evolution close to breakup. From (4.13) and (4.14) or (4.17), we deduce that $\Gamma \sim a$. Hence, the ratio of the leading-order viscous term F_μ in (4.12) to the leading-order term F_β arising from surface-tension gradients scales as

$$\frac{F_\mu}{F_\beta} \sim \frac{w/z^2}{\beta\Gamma/(az)} \sim \frac{1}{\beta\tau}. \tag{4.20}$$

Thus, as $\tau \to 0, F_\beta$ becomes negligible regardless of the strength of the surfactant. This is because the strong extensional flow in the neighbourhood of breakup sweeps

surfactant away from this region and $\Gamma \to 0$. Moreover, from (4.19) $\epsilon \sim \tau^{1/2} \to 0$ and the higher-order terms in (4.12) drop out. Thus, while the initial linear instability scales with σ_0 and is influenced by β, the final breakup scales with the uncontaminated surface tension $\sigma(0)$ and is unaffected by surfactant. (The same conclusion also applies to the intermediate asymptotic similarity solution for $\mathscr{R} \ll 1$ of Papageorgiou (1995) in which inertia is negligible, $z \sim \tau^{0.175}$, $w \sim \tau^{0.175-1}$, $a \sim \tau$ and (4.20) still holds.)

It is interesting to compare these theoretical scaling arguments with the numerical simulations of Ambravaneswaran & Basaran (1999) and Kwak & Pozrikidis (2001) which were based on the one-dimensional model (4.16) and boundary-integral calculations for Stokes flow respectively. Both papers allowed for surface diffusion of the insoluble surfactant and introduced a Péclet number to quantify the relative importance of advection and diffusion. For large Péclet numbers (small/negligible diffusion) the numerical results show the surfactant concentration approaching zero near pinching, in agreement with the theoretical arguments given here. Kwak & Pozrikidis (2001) also show numerical evidence for convergence towards the Stokes-flow similarity solution of Papageorgiou (1995).

For small Péclet numbers (rapid diffusion) the numerical results are more equivocal. Surfactant concentrations tended to decrease somewhere in the stretching neck, but not always at the narrowest point, and they were still far from zero when the calculations were terminated at a small, but non-zero, minimum radius. Nevertheless, we argue from (4.19) that extensional advection of surfactant asymptotically overwhelms diffusion so that the pinching region is again governed by the surfactant-free similarity solutions. (For diffusion to keep pace with advection, surfactant gradients would have to increase like $\tau^{-1/2}$, but both extension and diffusion act to reduce gradients.) Numerical confirmation of this argument would require higher-resolution calculations close to pinch-off.

4.4. *Long-wave evolution for $\beta > 1$*

In § 4.1, we argued that the long-wave model was accurate to $O(\epsilon^4)$ if $a\sigma' = O(a^2\bar{w}'')$. This condition ceases to hold for $\beta > 1$ and the accuracy of the model decreases to $O(\epsilon^2)$. Though the dominant activity is expected to shift to $O(1)$ wavelengths for $\beta > \frac{1}{2}$, it is instructive to consider the changed long-wave dynamics for $\beta > 1$. We make an alternative assumption that $a\sigma' \gg a^2\bar{w}''$ so that (4.5) and (4.7) become

$$(a\sigma)' = 0, \tag{4.21}$$

$$w_1 = \tfrac{1}{2}a\sigma', \tag{4.22}$$

at leading order. The axial force balance (4.21) is quasi-static and the average velocity $\bar{w}$ is determined instead by the surfactant transport equation

$$\dot{\Gamma} + (\bar{w} + \tfrac{1}{2}w_1)\Gamma' = -\tfrac{1}{2}\Gamma\{\bar{w}' + (aw_1)'/a\}. \tag{4.23}$$

Equations (4.21)–(4.23), together with (4.13), form a closed nonlinear model for this regime.

The characteristic equation for the linear stability problem is, as desired, the same as (3.11). The linearized equations also show that

$$w(r,z,t) = \left(\frac{3\beta - 1}{2\beta} + \frac{1-\beta}{\beta}\frac{r^2}{a^2}\right)\bar{w}(z,t), \tag{4.24}$$

so that w_1 and $\bar{w}$ are of comparable order rather than separated by $O(\epsilon^2)$. The quartic corrections are now $O(\epsilon^2)$ instead of $O(\epsilon^4)$ and, while (4.7), (4.12) and (4.14) include

(4.21)–(4.23) at leading order, the remaining terms are not the appropriate $O(\epsilon^2)$ corrections.

The mixture of parabolic and uniform flow in (4.24) corresponds to the same dynamical balance (between pressure gradients and shear stresses) as in standard lubrication theory, but with a partially slipping boundary condition. We note that $w(a)$ is generally non-zero, even as $\beta \to \infty$, in line with the conclusions of § 3.6.1.

5. Conclusion

We have examined various limiting forms of the characteristic equation relating growth rate α to wavenumber k for a periodically perturbed liquid thread in the presence of insoluble surfactant. As might be expected, surfactant slows the growth of the Rayleigh instability at all wavelengths and Reynolds numbers. However, increase of surfactant effects, as measured by a surface-tension-gradient parameter β, initiates a number of distinct transitions in the asymptotic behaviour.

First, we have shown that surfactant can act as a distinct mechanism for long-wave cut-off in the instability of a viscous thread. If $\beta < \frac{1}{2}$ then the cut-off is provided either by a small amount of inertia with $k \sim \mathscr{R}^{1/4}$ or by a small amount of external viscosity. In both cases k_m remains long-wave. However, if $\beta > \frac{1}{2}$ then k_m shifts toward $O(1)$ values, owing to the inhibition of axial motion by surfactant stresses.

Secondly, long-wave expansions reveal that $\beta = 1$ characterizes a transition from extensionally dominated flow with inertia for $\beta < 1$ to shear-dominated viscous flow with negligible inertia (like a lubrication flow) for $\beta > 1$. For $\beta > 1$, the viscous shear stresses are supported by surface-tension gradients and the axial velocity profile has comparable Poiseuille and plug-flow components.

In the limit $\beta \to \infty$, tangential flow must balance the local surface deformation so that the concentration of surfactant remains uniform on the surface; this condition means neither that the surface behaves rigidly nor that the surface tension is uniform, as is sometimes suggested. We have shown how this condition can be used to derive a characteristic equation relating growth rate and wavenumber in this limit.

Moving into the nonlinear regime, we have developed asymptotic expansions in a slenderness parameter ϵ leading to a one-dimensional model (4.24)–(4.14) for a surfactant-coated thread; unlike the case of a surfactant-free thread, such a model requires higher-order terms in addition to the full curvature even to give the same linear behaviour as the full axisymmetric equations, and a lower-order model can be quite misleading. There is surprisingly good agreement in linear growth rates between our one-dimensional model and the full equations over a wide range of wavenumbers and for different values of β. The model also includes the nonlinear terms necessary to capture the self-similar dynamics close to breakup: here scaling arguments show that surfactant is advected away from the point of breakup sufficiently rapidly that the asymptotic evolution in the absence of an external fluid is described by the equations and similarity solution for an uncontaminated thread (Eggers 1993; Brenner *et al.* 1996). How accurately the model describes the nonlinear evolution between the linear instability and the asymptotic similarity regime near breakup can only be evaluated properly by comparison with either experiments or high-resolution numerical simulations of the full axisymmetric equations. Such numerical comparisons have been made for the surfactant-free case (Wilkes, Phillips & Basaran 1999) by using a sophisticated adaptive finite-element method to resolve the two-dimensional flow at moderate Reynolds numbers, and it is hoped that a similar study will be made with surfactants. For applications, it would also be of interest to study the

formation, size and number of satellite drops, which depends on the global evolution from initial to final geometry. This is a tricky problem and previous studies with and without surfactants (Tjahjadi, Stone & Ottino 1992; Brenner, Shi & Nagel 1994; Ambravaneswaran & Basaran 1999; Kwak & Pozrikidis 2001, for example) have noted complex and non-monotonic behaviour, which makes it difficult to establish trends without an exhaustive parameter study.

Finally, we note that, even in this relatively simple problem, there is a rich asymptotic behaviour in which many of the limits do not commute. Some additional effects, such as surfactant diffusion or a small bulk solubility, would not be expected to change the long-wave behaviour, while adding the effects of a surrounding fluid of comparable viscosity certainly would. It is hoped that insights from the dynamical balances and asymptotic limits found in this problem can be used to guide further investigation of related problems, such as surfactant spreading.

REFERENCES

Abramovich, M. & Stegun, I. A. 1965 *Handbook of Mathematical Functions*, 3rd edn. Dover.

Ambravaneswaran, B. & Basaran, O. A. 1999 Effects of insoluble surfactants on the nonlinear deformation and breakup of stretching liquid bridges. *Phys. Fluids* **11**, 997–1015.

Bechtel, S. E., Carlson, C. D. & Forest, M. G. 1995 Recovery of the Rayleigh capillary instability from slender 1D inviscid and viscous models. *Phys. Fluids* **7**, 2956–2970.

Brenner, M. P., Lister, J. R. & Stone, H. A. 1996 Pinching threads, singularities and the number 0.0304. *Phys. Fluids* **8**, 2827–2836.

Brenner, M. P., Shi, X. D. & Nagel, S. R. 1994 Iterated instabilities during droplet fission. *Phys. Rev. Lett.* **73**, 3391–3394.

Eggers, J. 1993 Universal pinching of 3D axisymmetric free surface flows. *Phys. Rev. Lett.* **71**, 3458–3460.

Eggers, J. 1997 Nonlinear dynamics and breakup of free-surface flows. *Rev. Mod. Phys.* **69**, 865–929.

Eggers, J. & Dupont, T. F. 1994 Drop formation in a one-dimensional approximation of the Navier–Stokes equation. *J. Fluid Mech.* **262**, 205–221.

Garcia, F. J. & Castellanos, A. 1994 One-dimensional models for slender axisymmetric viscous liquid jets. *Phys. Fluids* A **6**, 2676–2689.

Hansen, S., Peters, G. W. M. & Meijer, H. E. E. 1999 The effect of surfactant on the stability of a fluid filament embedded in a viscous fluid. *J. Fluid Mech.* **382**, 331–349.

Kwak, S. & Pozrikidis, C. 2001 Effect of surfactants on the instability of a liquid thread or annular layer. Part 1: Quiescent fluids. *Intl J. Multiphase Flow* **27**, 1–37.

Lister, J. R., Brenner, M. P., Stone, H. A., Day, R. F. & Hinch, E. J. 1997 Singularities and similarity solutions in capillary breakup. In *Proc. IUTAM Symposium on Nonlinear Singularities in Deformation and Flow, Haifa* (ed. D. Durban & J. R. A. Pearson), pp. 257–269. Kluwer.

Lister, J. R. & Stone, H. A. 1998 Capillary breakup of a viscous thread surrounded by another viscous fluid. *Phys. Fluids* **10**, 2758–2764.

Milliken, W. J., Stone, H. A. & Leal, L. G. 1993 The effect of surfactant on the transient motion of newtonian drops. *Phys. Fluids* A **5**, 69–79.

Palierne, J. F. & Lequeux, F. 1991 Sausage instability of a thread in a matrix; linear theory for viscoelastic fluids and interface. *J. Non-Newtonian Fluid Mech.* **40**, 289–306.

Papageorgiou, D. T. 1995 On the breakup of viscous liquid threads. *Phys. Fluids* **7**, 1529–1544.

Rayleigh, Lord 1879 On the instability of jets. *Proc. Lond. Math. Soc.* **10**, 4.

Rayleigh, Lord 1892 On the stability of a cylinder of viscous liquid under capillary force. *Phil. Mag.* **34**, 145.

Stone, H. A. 1990 A simple derivation of the time-dependent convective-diffusion equation for surfactant transport along a deforming interface. *Phys. Fluids* A **2**, 111–112.

Stone, H. A. & Leal, L. G. 1990 The effects of surfactants on drop deformation and breakup. *J. Fluid Mech.* **220**, 161–186.

Tjahjadi, M. & Ottino, J. 1991 Stretching and breakup of droplets in chaotic flows. *J. Fluid Mech.* **232**, 191–219.

Tjahjadi, M., Stone, H. A. & Ottino, J. M. 1992 Satellite and subsatellite formation in capillary breakup. *J. Fluid Mech.* **243**, 297–317.

Tomotika, S. 1935 On the stability of a cylindrical thread of a viscous liquid surrounded by another viscous fluid. *Proc. R. Soc. Lond.* A **150**, 322.

Tricot, Y.-M. 1997 Surfactants: static and dynamic surface tension. In *Liquid Film Coating* (ed. S. F. Kistler & P. M. Schweizer), pp. 100–136. Chapman & Hall.

Whitaker, S. 1976 Studies of drop-weight method for surfactant solutions III. Drop stability, the effect of surfactants on the stability of a column of liquid. *J. Colloid Interface Sci.* **54**, 231–248.

Wilkes, E. D., Phillips, S. D. & Basaran, O. A. 1999 Computational and experimental analysis of drop formation. *Phys. Fluids* A **11**, 3577–3598.

Zhang, X., Padgett, R. S. & Basaran, O. A. 1996 Nonlinear deformation and breakup of stretching liquid bridges. *J. Fluid Mech.* **329**, 207.